Available online at www.sciencedirect.com

ScienceDirect

IFAC PapersOnline CONFERENCE PAPER ARCHIVE

IFAC PapersOnLine 56-2 (2023) 10880–10885

Fault Diagnosis For Wave Energy Converters With Model Uncertainties

Yao Zhang * **Tianyi Zeng** ** **Zhiwei Gao** *** **Stephen Turnock** * **Dominic Hudson** *

* *School of Engineering, University of Southampton, Boldrewood Innovation Campus, SO16 7QF, UK, (e-mail: yao.zhang,S.R.Turnock, Dominic@soton.ac.uk).*

** *Rolls-Royce UTC in Manufacturing and On-wing Technology, University of Nottingham, NG8 1BB, UK,(e-mail: Tianyi.Zeng@nottingham.ac.uk)*

*** *Faculty of Engineering and Environment, University of Northumbria, Newcastle upon Tyne, NE1 8ST, UK (e-mail: Zhiwei.Gao @northumbria.ac.uk)*

Abstract: Unexpected sensor and actuator faults degrade the control performance and even introduce damage breaking down the wave energy converter (WEC) system. Fault detection for wave energy converters is of great importance in enhancing the reliability and robustness of WECs. This paper investigates a robust fault diagnosis method for single-point absorbers. An unknown input observer is designed to estimate the fault in real-time, which is robust against model uncertainties. This method can also be straightforwardly applied to other types of WEC. The parameters of the proposed observer can be calculated offline, which enhances the real-time implementation with a low computational burden.

Keywords: Fault diagnosis, Wave energy converters, Robustness, Unknown input observer

1. INTRODUCTION

As a promising renewable and clean energy resource, sea wave has the potential to contribute to carbon emission reduction and generate a considerable amount of electricity, e.g. 20 percent of UK electricity. However, wave energy has not been widely commercialized due to high unit costs and maintenance costs (Ringwood et al. (2014); Drew et al. (2009)), which leads to the demand for research on advanced control strategies.

To harness wave energy, multiple types of wave energy converters (WECs) have been developed. As a benchmark problem, the point absorber WEC is usually chosen to demonstrate the efficacy of the control in the initial stage. Unlike control objectives in aerospace systems or marine operation systems, which mainly aim at stabilizing the system, the control objective in WEC control is to maximize the energy output. The energy maximization of point absorber WECs is usually achieved by optimizing the control signal actuated by the power take-off (PTO).

It has been long recognized that effective control can at least double the energy output (Ringwood et al. (2014)). It has also been recognized that WEC control is a non-causal optimal control problem (Ringwood et al. (2014); Falnes (2002)), in which the current control action is determined by the future information of sea waves. Compared with the causal control, the non-causal control which incorporates the prediction of the incoming wave significantly improves WEC control performance (see Hals et al. (2011); Zhang et al. (2020a); Genest and Ringwood (2016); Ringwood et al. (2014)).

Several categories of non-causal control methods have been proposed for WECs to tackle different control problems. To tackle the constraints in WEC operations, including limited float position and velocity as well as limited PTO actuators, model predictive control (MPC) has been designed to solve the constrained optimization problem (Brekken (2011); Richter et al. (2012); Son and Yeung (2017)). For WECs with partially unknown models, adaptive dynamic programming (ADP) was proposed to simultaneously find solutions to the control action and the optimized cost function (Na et al. (2018); Zhan et al. (2019)), and deep learning based control was proposed to get the insight of the model which provides efficient control performance (Li et al. (2018)). To cope with model uncertainties, robust control was designed to maximize the energy output subject to bounded model mismatch (Schoen et al. (2011)). To consider the un-measurable states and wave forces which are required by the controller, Kalman Filter and sliding mode observer have been designed to provide an estimate of related variables (Garcia-Abril et al. (2017); Zhang et al. (2020b)). To investigate the control degradation caused by prediction errors, a sensitivity model of non-causal control to excitation force prediction error was proposed (Fusco and Ringwood (2011)), and a sliding mode technique was exploited to cope with the prediction error (Zhang et al. (2020c)).

Current control methods mainly assume that actuators and sensors do not contain any faults, which means the

10.1016/j.ifacol.2023.10.767

control signal can be actuated by the PTO and the measurement from sensors can be relied on. However, considering seawater corrosion, mechanical failure, and unexpected damages from marine organism, we need to take into account that the sensors and actuators in WEC systems may not function well, which degrades the control performance and even breaks down the whole system. Therefore, it is of vital importance to design a fault diagnosis method so that the controller is aware of such faults.

The fault diagnosis method has been successfully applied to mechanical systems, aerospace systems, and many other systems (Chen and Patton (2012); Edwards et al. (2000); Gao et al. (2007)). Very recently, research on fault diagnosis for WEC has been undertaken (González-Esculpi et al. (2022); Xu et al. (2022); Zhang et al. (2022)). While the model uncertainty caused by unmodelled wave forces and state-space model approximations is not fully considered.

The fault is usually coupled with the model uncertainty, which brings a challenge to the fault diagnosis. This paper aims to investigate a robust fault diagnosis method subject to model uncertainties. This is achieved by designing a robust unknown input observer (UIO) with extended states that are not sensitive to the external disturbances.

The rest of the paper is organized as follows. Section 2 introduces a state-space model of the single point absorber, where sensor faults and actuator faults are considered. The fault detection method is proposed in Section 3, where the stability is proven. Simulation results are shown in Section 4. Section 5 concludes this paper. In this paper, $\|x\|$ denotes the norm of vector x, while $\|x\|_t = \sqrt{\int_0^t x^{\mathrm{T}}(\tau)x(\tau)d\tau}$, and $\begin{bmatrix} M_1 & M_2 \\ \star & M_3 \end{bmatrix} = \begin{bmatrix} M_1 & M_2 \\ M_2^{\mathrm{T}} & M_3 \end{bmatrix}$.

2. WEC MODEL

In this section, the dynamic model and the state-space model of WEC are introduced, in which both the model uncertainty and the faults are considered.

2.1 Dynamic model of WEC

Fig. 1 shows part of a hydraulic power take-off (PTO) design: a hydraulic cylinder is vertically installed below the float and is fixed to the bottom of the seabed. The single point absorber is constrained to heave motion only. z_v is the displacement of the mid-point of the float. The PTO force denoted as f_u represents the piston force. The extracted power is $P := -f_u\dot{z}_v$.

By using Newton's second law, the dynamic equation for the float of the point absorber is

$$m_s\ddot{z}_v = -f_s - f_r + f_e + f_u \tag{1}$$

where m_s is the float mass; the restoring force f_s is given by

$$f_s = k_s z_v \tag{2}$$

with the hydrostatic stiffness $k_s = \rho g s$, and ρ as water density, g as standard gravity, and s as the cross-sectional area of the float. f_r is the radiation force determined by

$$f_r = m_\infty\ddot{z}_v + \int_{-\infty}^{\infty} h_r(\tau)\dot{z}_v(t-\tau)d\tau \tag{3}$$

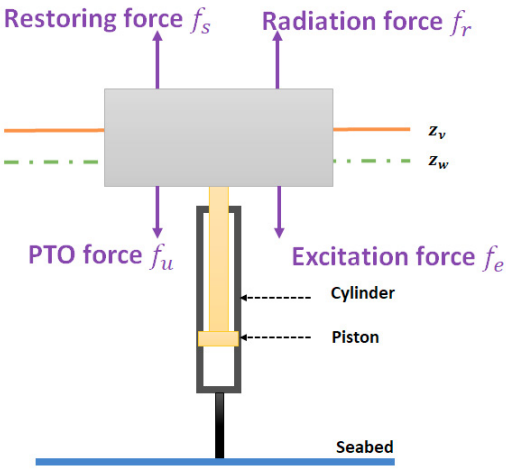

Fig. 1. Schematic diagram of the point absorber

where m_∞ is the added mass; h_r is the kernel of the radiation force that can be computed via hydraulic software packages (e.g. WAMIT Lee (1995)). Following Yu and Falnes (1995), the convolutional term in (3) $f_R := \int_{-\infty}^{\infty} h_r(\tau)\dot{z}_v(t-\tau)d\tau$ can be approximated by a causal finite dimensional state-space model

$$\dot{x}_r = A_r x_r + B_r\dot{z}_v \tag{4a}$$

$$f_R = C_r x_r \approx \int_{-\infty}^{t} h_r(\tau)\dot{z}_v(t-\tau)d\tau \tag{4b}$$

where $(A_r,\ B_r\ C_r,\ 0)$ and $x_r \in \mathbb{R}^{n_r}$ are the state-space realization and the state respectively. Similarly, the wave excitation force can be written as

$$f_e = \int_{-\infty}^{\infty} h_e(\tau)\dot{z}_w(t-\tau)d\tau \tag{5}$$

where z_w is the wave elevation, and the state-space approximation is

$$\dot{x}_e = A_e x_e + B_e\dot{z}_w \tag{6a}$$

$$f_e = C_e x_e \approx \int_{-\infty}^{t} h_e(\tau)z_w(t-\tau)d\tau \tag{6b}$$

where $(A_e,\ B_e,\ C_e,\ 0)$ and $x_e \in \mathbb{R}^{n_e}$ are the state-space realization and the state, and n_r and n_e are dimensions of the radiation state and the excitation state.

2.2 State-space model with faults and model uncertainties

To avoid possible damages or control performance degradation caused by sensor faults and actuator faults, a fault vector is considered in the model. Moreover, the model uncertainties denoted as ϵ are also included in the model to reflect realistic scenarios. The fault vector is defined as $f \in \mathbb{R}^{3\times 1}$, which involves two sensor faults (displacement sensor fault and velocity sensor fault) and a PTO actuator fault. The wave elevation z_w and the model uncertainties $\epsilon \in \mathbb{R}^{n_\epsilon\times 1}$ with $n_\epsilon > 0$ being the dimension of model uncertainties are lumped into the disturbance term $d = \begin{bmatrix} z_w & \epsilon^{\mathrm{T}} \end{bmatrix}^{\mathrm{T}}$, and the former is to be decoupled and the latter cannot be fully decoupled.

Define the state vector as

$$x = [z_v, \dot{z}_v, x_r, x_e] \in \mathbb{R}^{(n_r+n_e+2)\times 1} \tag{7}$$

Define the control input as

$$u = f_u \tag{8}$$

The continuous-time state-space model considering both model uncertainties and faults is as follows

$$\begin{cases} \dot{x} = & Ax + B_u u + B_d d + B_f f \\ y = & Cx + D_f f \end{cases} \tag{9}$$

where

$$A = \begin{bmatrix} 0 & 1 & 0 & 0 \\ -\frac{k_s}{m} & 0 & -\frac{C_r}{m} & \frac{C_e}{m} \\ 0 & B_r & A_r & 0 \\ 0 & 0 & 0 & A_e \end{bmatrix} \in \mathbb{R}^{(n_r+n_e+2)\times(n_r+n_e+2)}$$

$$B_u = \begin{bmatrix} 0 & \frac{1}{m} & 0 & 0 \end{bmatrix}^{\mathrm{T}}, \quad C = \begin{bmatrix} 1 & 0 & 0_{1\times(n_r+n_e)} \\ 0 & 1 & 0_{1\times(n_r+n_e)} \end{bmatrix}$$

$$B_d = [B_{d1} \ B_{d2}], \quad B_{d1} = [0 \ 0 \ 0 \ B_e]^{\mathrm{T}}$$

with $m := m_s + m_\infty$, and the disturbance related matrix B_{d2} and the fault related matrices B_f and D_f are known constant matrices with appropriate dimensions.

3. ROBUST FAULT DIAGNOSIS

In this section, an augmented system is first constructed, based on which an observer is designed to detect the sensor/actuator faults. The stability and robustness are proven. The design procedure is introduced to provide a guide for the implementation of the proposed observer.

3.1 Augmented System

We consider incipient or abrupt faults in WEC systems, which leads to $\ddot{f} = 0$. Define an augmented state as

$$\bar{x} = \begin{bmatrix} x^{\mathrm{T}} & \dot{f}^{\mathrm{T}} & f^{\mathrm{T}} \end{bmatrix}^{\mathrm{T}} \tag{10}$$

By the state-space model (9), we have the following augmented system

$$\begin{cases} \dot{\bar{x}} = & \bar{A}\bar{x} + \bar{B}_u u + \bar{B}_d d \\ y = & \bar{C}\bar{x} \end{cases} \tag{11}$$

where

$$\begin{aligned} \bar{A} &= \begin{bmatrix} A & 0 & B_f \\ 0 & 0 & 0 \\ 0 & I_3 & 0 \end{bmatrix} \in \mathbb{R}^{(n_r+n_e+8)\times(n_r+n_e+8)} \\ \bar{B}_u &= \begin{bmatrix} B_u \\ 0 \\ 0 \end{bmatrix}, \quad \bar{B}_d = \begin{bmatrix} B_d \\ 0 \\ 0 \end{bmatrix}, \quad \bar{C} = [C \ 0 \ D_f] \end{aligned} \tag{12}$$

3.2 Fault diagnosis with model uncertainties

This subsection is to design an unknown input observer to estimate the augmented state vector $\bar{x}$ based on the augmented system (11), and the concerned fault vector f, as well as its first time-derivative $\dot{f}$, are therefore to be precisely estimated.

The estimation error is defined as

$$\bar{e} = \bar{x} - \hat{\bar{x}} \tag{13}$$

where $\hat{\bar{x}}$ is the estimate of the state vector $\bar{x}$. The observer is designed as follows

$$\begin{cases} \hat{\bar{x}} = & \psi + Hy \\ \dot{\psi} = & R\psi + G\bar{B}_u u + Ky \end{cases} \tag{14}$$

where $\psi \in \mathbb{R}^{n_r+n_e+8}$ is an auxiliary variable, and $H \in \mathbb{R}^{(n_r+n_e+8)\times 2}$, $R \in \mathbb{R}^{(n_r+n_e+8)\times(n_r+n_e+8)}$, $G \in \mathbb{R}^{(n_r+n_e+8)\times(n_r+n_e+8)}$ and $K \in \mathbb{R}^{(n_r+n_e+8)\times 2}$ are coefficient matrices of the observer, which are to be designed to ensure the existence of the observer. $K = K_1 + K_2$, where $K_1 \in \mathbb{R}^{(n_r+n_e+8)\times(n_r+n_e+8)}$ and $K_2 \in \mathbb{R}^{(n_r+n_e+8)\times(n_r+n_e+8)}$ are constant matrices.

The estimation error can be rewritten as

$$\bar{e} = \bar{x} - \psi - Hy = -\psi + (I_{(n_r+n_e+8)} - H\bar{C})\bar{x} \tag{15}$$

From (14) and (11), its derivative is

$$\begin{aligned} \dot{\bar{e}} =& -\dot{\psi} + (I_{(n_r+n_e+8)} - H\bar{C})\dot{\bar{x}} \\ =& -R\psi - G\bar{B}_u u - K_1\bar{C}\bar{x} - K_2 y \\ & + (I_{(n_r+n_e+8)} - H\bar{C})(\bar{A}\bar{x} + \bar{B}_u u + \bar{B}_d d) \\ =& (\bar{A} - H\bar{C}\bar{A} - K_1\bar{C})\bar{e} \\ & + (\bar{A} - H\bar{C}\bar{A} - K_1\bar{C} - R)\psi \\ & + [(\bar{A} - H\bar{C}\bar{A} - K_1\bar{C})H - K_2]y \\ & + [(I_{(n_r+n_e+8)} - H\bar{C})\bar{B}_u - G\bar{B}_u]u \\ & + (I_{(n_r+n_e+8)} - H\bar{C})\bar{B}_{d1} z_w \\ & + (I_{(n_r+n_e+8)} - H\bar{C})\bar{B}_{d2}\epsilon \end{aligned} \tag{16}$$

where $\begin{bmatrix} \bar{B}_{d1} & \bar{B}_{d2} \end{bmatrix} = \bar{B}_d$.

From (16), the estimation error dynamics can be reduced as

$$\dot{\bar{e}} = R\bar{e} + (I_{(n_r+n_e+8)} - H\bar{C})\bar{B}_{d2}\epsilon \tag{17}$$

if the following equations hold

$$R = \bar{A} - H\bar{C}\bar{A} - K_1\bar{C} \tag{18}$$

$$K_2 = RH \tag{19}$$

$$G = I_{(n_r+n_e+8)} - H\bar{C} \tag{20}$$

$$(I_{(n_r+n_e+8)} - H\bar{C})\bar{B}_{d1} = 0 \tag{21}$$

From (17), the wave elevation z_w is decoupled with the conditions (18) $\sim$ (21), and the model uncertainties ϵ exists in the estimation error dynamics. The objective becomes seeking the solutions of (21) and simultaneously minimizing the influence from ϵ.

Lemma 1. The existence of the proposed observer (14) is guaranteed by the following conditions (see Chen et al. (1996); Gao et al. (2015) for details):

- $\mathrm{rank}(\bar{C}\bar{B}_{d1}) = \mathrm{rank}(\bar{B}_{d1})$;
- $(\bar{C}, \bar{A}_1)$ is detectable, where $\bar{A}_1 = (I_{(n_r+n_e+8)} - H\bar{C})\bar{A}$. With these conditions, (21) is solvable, and a special solution is

$$H^* = \bar{B}_{d1}[(\bar{C}\bar{B}_{d1})^{\mathrm{T}}(\bar{C}\bar{B}_{d1})]^{-1}(\bar{C}\bar{B}_{d1})^{\mathrm{T}} \tag{22}$$

Theorem 2. For the augmented system (11), the estimation error satisfies $\|\bar{e}\|_{t_f} \le \gamma\|\epsilon\|_{t_f}$ by the proposed observer (14) if there exist positive definite matrices P and Q such that

$$\begin{bmatrix} I + \bar{A}_1^{\mathrm{T}}P + P\bar{A}_1 - \bar{C}^{\mathrm{T}}Q^{\mathrm{T}} - Q\bar{C} & P(I - H\bar{C})\bar{B}_{d2} \\ \star & -\gamma^2 I \end{bmatrix} < 0 \tag{23}$$

holds, where $\bar{A}_1 = (I_{(n_r+n_e+8)} - H_{ob}\bar{C})\bar{A}$ and $Q = PK_1$.

Proof. See Appendix A.

3.3 Implementation

The parameters in (14) can be designed by following steps.

- Step 1: Determine the system matrices $\bar{A}$, $\bar{B}_u$, $\bar{B}_d$, $\bar{C}$ in the augmented system (11) by using (12);

- Step 2: Solve the special solution of H by using (22);
- Step 3: Obtain Q and P by solving the linear matrix inequality (LMI) (23) ;
- Step 4: Obtain the gain by using $K_1 = P^{-1}Q$;
- Step 5: Obtain the other gains R, G, K_2 and K by using (18) $\sim$ (21) and $K = K_1 + K_2$.

The estimated augmented state $\hat{\bar{x}}$ can be obtained by (14), and the state and fault can be simultaneously estimated by

$$\hat{x} = \left[I_{(n_r+n_e+2)} \ 0_{(n_r+n_e+2)\times 6}\right] \hat{\bar{x}} \tag{24}$$

and

$$\hat{f} = \left[0_{3\times(n_r+n_e+5)} \ I_3\right] \hat{\bar{x}} \tag{25}$$

4. SIMULATION RESULTS

Matlab 2012b is used in simulation with sampling period as $t = 0.1$ s. The parameters of the WEC model and the hydrodynamic coefficients are adopted from those used in Yu and Falnes (1995). The parameters of single point absorber are shown in Table 1. The stiffness is $k_s = 3866$ N/m, the float mass is $m_s = 242$ kg, and the added mass is $m_\infty = 83.5$ kg. The state-space matrices of the impulse function for calculating the radiation force (Yu and Falnes (1995)) is

$$A_r = \begin{bmatrix} 0 & 0 & -17.9 \\ 1 & 0 & -17.7 \\ 0 & 1 & -4.41 \end{bmatrix}, B_r = \begin{bmatrix} 36.5 \\ 394 \\ 75.1 \end{bmatrix}, C_r = [0 \ 0 \ 1]$$

The state-space matrices of the impulse function for calculating the excitation force (Yu and Falnes (1995)) is

$$A_e = \begin{bmatrix} 0 & 0 & 0 & 0 & -400 \\ 1 & 0 & 0 & 0 & -459 \\ 0 & 1 & 0 & 0 & -226 \\ 0 & 0 & 1 & 0 & -64 \\ 0 & 0 & 0 & 1 & -9.96 \end{bmatrix}, B_e = \begin{bmatrix} 1549886 \\ -116380 \\ 24748 \\ -644 \\ 19.3 \end{bmatrix}$$

$$C_e = [0 \ 0 \ 0 \ 0 \ 1]$$

Table 1. Single Point Absorber Parameters

Description	Notation	values
Stiffness	k_s	3866 N/m
Float mass	m_s	242 kg
Added mass	m_∞	83.5 kg
Total mass	m	325.5 kg

The model uncertainty is considered as zero mean white Gaussian noises $\mathcal{N} \sim (0, 0.3)$. The displacement sensor fault is considered as

$$f = \begin{cases} 0, & 0 \le t < 20, 30 \le t \le 40 \\ 0.1t - 2, & 20 \le t < 25 \\ 3 - 0.1t, & 25 \le t < 30 \end{cases}$$

The velocity sensor fault is considered as

$$f = \begin{cases} 0, & 0 \le t < 10, 30 \le t \le 40 \\ -0.1t + 1, & 20 \le t < 25 \\ -3 + 0.1t, & 25 \le t < 30 \end{cases}$$

The PTO actuator sensor fault is considered as

$$f = \begin{cases} \sin(0.1t), & 0 \le t < 20 \\ 0.2, & 20 \le t < 30 \\ -0.1, & 30 \le t \le 40 \end{cases}$$

The actual fault signal and its estimate achieved by the proposed observer and the estimation error are shown in Figs. 2, 3 and 4, in which it can be found that the proposed observer estimates the actual fault precisely with the maximum estimation error as 0.06 (11% of the peak value in actual signal). The real time fault detection is therefore effective.

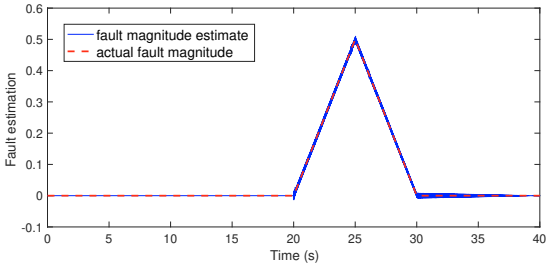

Fig. 2. Displacement sensor fault and its estimation

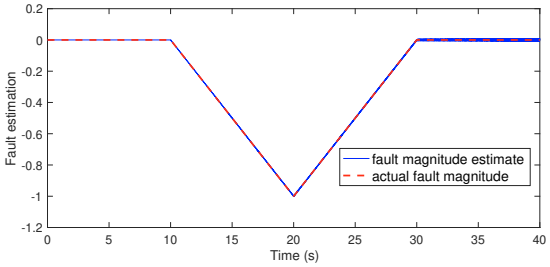

Fig. 3. Velocity sensor fault and its estimation

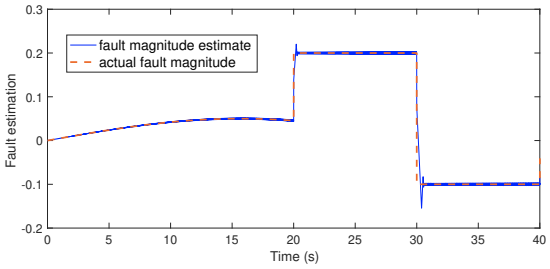

Fig. 4. PTO actuator fault and its estimation

5. CONCLUSION

An unknown input observer was proposed to detect sensor and actuator faults for wave energy converters. The proposed observer was proven to be stable and robust against the model uncertainty. Simulation results showed the proposed observer was efficient and effective in detecting faults. The parameters of proposed observer are offline calculated, which enhance the real-time implementation with a low computational burden. Future works will be applications to multi-float multi-mode-motion wave energy converters.

6. ACKNOWLEDGEMENT

This work was supported by Maritime Engineering Group, University of Southampton and Young Scientists Fund of the National Natural Science Foundation of China (Grant No. 62203219).

REFERENCES

Brekken, T.K. (2011). On model predictive control for a point absorber wave energy converter. In *2011 IEEE Trondheim PowerTech*, 1–8. IEEE.

Chen, J. and Patton, R.J. (2012). *Robust model-based fault diagnosis for dynamic systems*, volume 3. Springer Science & Business Media.

Chen, J., Patton, R.J., and Zhang, H.Y. (1996). Design of unknown input observers and robust fault detection filters. *International Journal of control*, 63(1), 85–105.

Drew, B., Plummer, A.R., and Sahinkaya, M.N. (2009). A review of wave energy converter technology.

Edwards, C., Spurgeon, S.K., and Patton, R.J. (2000). Sliding mode observers for fault detection and isolation. *Automatica*, 36(4), 541–553.

Falnes, J. (2002). *Ocean waves and oscillating systems: linear interactions including wave-energy extraction*. Cambridge university press.

Fusco, F. and Ringwood, J. (2011). A model for the sensitivity of non-causal control of wave energy converters to wave excitation force prediction errors. In *Proceedings of the 9th European Wave and Tidal Energy Conference (EWTEC)*. School of Civil Engineering and the Environment, University of Southampton.

Gao, Z., Breikin, T., and Wang, H. (2007). High-gain estimator and fault-tolerant design with application to a gas turbine dynamic system. *IEEE Transactions on Control Systems Technology*, 15(4), 740–753.

Gao, Z., Liu, X., and Chen, M.Z. (2015). Unknown input observer-based robust fault estimation for systems corrupted by partially decoupled disturbances. *IEEE Transactions on Industrial Electronics*, 63(4), 2537–2547.

Garcia-Abril, M., Paparella, F., and Ringwood, J.V. (2017). Excitation force estimation and forecasting for wave energy applications. *IFAC-PapersOnLine*, 50(1), 14692–14697.

Genest, R. and Ringwood, J.V. (2016). A critical comparison of model-predictive and pseudospectral control for wave energy devices. *Journal of Ocean Engineering and Marine Energy*, 2(4), 485–499.

González-Esculpi, A., Verde, C., and Maya-Ortiz, P. (2022). Comparison of estimates of the excitation force for fault diagnosis in a wave energy converter. *IFAC-PapersOnLine*, 55(6), 396–401.

Hals, J., Falnes, J., and Moan, T. (2011). Constrained optimal control of a heaving buoy wave-energy converter. *Journal of Offshore Mechanics and Arctic Engineering*, 133(1), 011401.

Lee, C.H. (1995). *WAMIT theory manual*. Massachusetts Institute of Technology, Department of Ocean Engineering.

Li, L., Yuan, Z., and Gao, Y. (2018). Maximization of energy absorption for a wave energy converter using the deep machine learning. *Energy*, 165, 340–349.

Na, J., Wang, B., Li, G., Zhan, S., and He, W. (2018). Nonlinear constrained optimal control of wave energy converters with adaptive dynamic programming. *IEEE Transactions on Industrial Electronics*, 66(10), 7904–7915.

Richter, M., Magana, M.E., Sawodny, O., and Brekken, T.K. (2012). Nonlinear model predictive control of a point absorber wave energy converter. *IEEE Transactions on Sustainable Energy*, 4(1), 118–126.

Ringwood, J.V., Bacelli, G., and Fusco, F. (2014). Energy-maximizing control of wave-energy converters: The development of control system technology to optimize their operation. *IEEE control systems magazine*, 34(5), 30–55.

Schoen, M.P., Hals, J., and Moan, T. (2011). Wave prediction and robust control of heaving wave energy devices for irregular waves. *IEEE Transactions on energy conversion*, 26(2), 627–638.

Son, D. and Yeung, R.W. (2017). Optimizing ocean-wave energy extraction of a dual coaxial-cylinder wec using nonlinear model predictive control. *Applied energy*, 187, 746–757.

Xu, N., Chen, L., Yang, R., and Zhu, Y. (2022). Multi-controller-based fault tolerant control for systems with actuator and sensor failures: Application to 2-body point absorber wave energy converter. *Journal of the Franklin Institute*, 359(12), 5919–5934.

Yu, Z. and Falnes, J. (1995). State-space modelling of a vertical cylinder in heave. *Applied Ocean Research*, 17(5), 265–275.

Zhan, S., Na, J., and Li, G. (2019). Nonlinear noncausal optimal control of wave energy converters via approximate dynamic programming. *IEEE Transactions on Industrial Informatics*, 15(11), 6070–6079.

Zhang, Y., Stansby, P., and Li, G. (2020a). Non-causal linear optimal control with adaptive sliding mode observer for multi-body wave energy converters. *IEEE Transactions on Sustainable Energy*, 12(1), 568–577.

Zhang, Y., Zeng, T., and Gao, Z. (2022). Fault diagnosis and fault-tolerant control of energy maximization for wave energy converters. *IEEE Transactions on Sustainable Energy*, 13(3), 1771–1778. doi: 10.1109/TSTE.2022.3174781.

Zhang, Y., Zeng, T., and Li, G. (2020b). Robust excitation force estimation and prediction for wave energy converter m4 based on adaptive sliding-mode observer. *IEEE Transactions on Industrial Informatics*, 16(2), 1163–1171. doi:10.1109/TII.2019.2941886.

Zhang, Y., Zhan, S., and Li, G. (2020c). Model predictive control of wave energy converters with prediction error tolerance. *IFAC-PapersOnLine*, 53(2), 12289–12294.

Appendix A. PROOF OF THEOREM

Select a Lyapunov candidate as $V = \bar{e}^{\mathrm{T}} P \bar{e}$. Its first time derivative is

$$\dot{V} = \bar{e}^{\mathrm{T}} P \dot{\bar{e}} + \dot{\bar{e}}^{\mathrm{T}} P \bar{e} \tag{A.1}$$

From (17) and (18), we can rewrite (A.1) as

$$\begin{aligned} \dot{V} =& \bar{e}^{\mathrm{T}} (\bar{A}_1^{\mathrm{T}} P + P \bar{A}_1 - \bar{C}^{\mathrm{T}} Q^{\mathrm{T}} - Q \bar{C}) \bar{e} \\ &+ 2 \bar{e}^{\mathrm{T}} P (I - H \bar{C}) \bar{B}_{d2} \epsilon \end{aligned} \tag{A.2}$$

From the condition (23) in Theorem 2, we have

$$\bar{A}_1^{\mathrm{T}} P + P \bar{A}_1 - \bar{C}^{\mathrm{T}} Q^{\mathrm{T}} - Q \bar{C} < -I < 0 \tag{A.3}$$

which means $\dot{V} < 0$ holds if $\epsilon = 0$. Since the model uncertainties ϵ is assumed to be bounded, so the estimation error is asymptotically stable.

Define a new variable as

$$\Theta = \int_0^{t_f} (\bar{e}^{\mathrm{T}} \bar{e} - \gamma^2 \epsilon^{\mathrm{T}} \epsilon) dt \tag{A.4}$$

We now prove that $\Theta < 0$, which leads to $\|\bar{e}\|_{t_f} \leq \gamma \|\epsilon\|_{t_f}$.

From (A.2), we have

$$\begin{aligned}\Theta &= \int_0^{t_f} (\bar{e}^{\mathrm{T}}\bar{e} - \gamma^2\epsilon^{\mathrm{T}}\epsilon + \dot{V})dt - \int_0^{t_f} \dot{V}dt \\ &= \int_0^{t_f} [\bar{e}^{\mathrm{T}}(I + \bar{A}_1^{\mathrm{T}}P + P\bar{A}_1 - \bar{C}^{\mathrm{T}}Q^{\mathrm{T}} - Q\bar{C})\bar{e}]dt \\ &\quad + \int_0^{t_f} [2\bar{e}^{\mathrm{T}}P(I - H\bar{C})\bar{B}_{d2}\epsilon - \gamma^2\epsilon^{\mathrm{T}}\epsilon]dt \\ &\quad - \int_0^{t_f} \dot{V}dt \\ &= \int_0^{t_f} \begin{bmatrix}\bar{e}^{\mathrm{T}} & \epsilon^{\mathrm{T}}\end{bmatrix} \Phi \begin{bmatrix}\bar{e} \\ \epsilon\end{bmatrix} dt - \int_0^{t_f} \dot{V}dt\end{aligned} \tag{A.5}$$

where

$$\Phi = \begin{bmatrix} I + \bar{A}_1^{\mathrm{T}}P + P\bar{A}_1 - \bar{C}^{\mathrm{T}}Q^{\mathrm{T}} - Q\bar{C} & P(I - H\bar{C})\bar{B}_{d2} \\ \star & -\gamma^2 I \end{bmatrix}$$

The initial condition is assumed to be $\bar{e}(0) = 0$, which gives

$$\int_0^{t_f} \dot{V}dt = \bar{e}^{\mathrm{T}}(t_f)P\bar{e}(t_f) - \bar{e}^{\mathrm{T}}(0)P\bar{e}(0) = V(\bar{e}(t_f)) > 0 \tag{A.6}$$

From (23), we have $\Phi < 0$, and from (A.5) and (A.6), we have $\Theta < 0$, which leads to $\|\bar{e}\|_{t_f} \leq \gamma\|\epsilon\|_{t_f}$. This completes the proof.